# Microstructure and Hardness of Hollow Cathode Discharge Ion-Plated Titanium Nitride Film

*C.T. Chen, Y.C. Song, G.-P. Yu, and J.-H. Huang*

*(Submitted 6 November 1997; in revised form 23 January 1998)*

**Titanium nitride (TiN) films were deposited on 304 stainless steel substrate by hollow cathode discharge (HCD) ion-plating technique. The preferred orientation and microstructure were studied by x-ray diffraction (XRD) and transmission electron microscopy (TEM), respectively. Microhardness of the TiN film was measured and correlated to the microstructure and preferred orientation. The results of TEM study showed that the microstructure of TiN film contains grains with nanometer scale. As the film thickness increases, the grain size of TiN increases. The x-ray results show that TiN(111) is the major preferred orientation of the film. The hardness of TiN film is primarily contributed from TiN(111) preferred orientation.**

**Keywords** coatings, hollow cathode discharge, TiN, type 304

## 1. Introduction

Due to excellent mechanical properties and corrosion resistance, titanium nitride (TiN) is commercially used on steels as a protection film to extend the life of the steels. Hardness is a simple and convenient index employed to evaluate the mechanical property of TiN film. The hardness of TiN film varies from 340 to 3000 kgf/mm$^2$, depending on deposition technique and deposition parameters (Ref 1). Among the various deposition techniques for producing TiN, ion plating is unique in providing better adhesion between coating and substrate than other techniques (Ref 2-4). Hollow cathode discharge (HCD) ion plating is one of the most popular techniques used in industry for thin film preparation.

Many factors can affect the hardness of TiN films. One of the important factors is the microstructure of thin film. The microstructure and mechanical properties of TiN vary with processing and deposition conditions. In reality, even small changes in the composition or structure of films can lead to wide differences in the properties of TiN film (Ref 5). Although engineering aspects of the ion-plating technique and resulting coating properties have been studied extensively (Ref 4, 6-7), the microstructure, such as grain size, preferred orientation, and the relation to hardness of TiN film have not been investigated in great detail.

The purpose of this study is to investigate the relationship between hardness and microstructure, including grain size and preferred orientation of TiN film produced by HCD method.

## 2. Experiment

The substrate material for TiN coating was commercial 304 stainless steel (304 SS) plate with dimensions of 30 by 30 by 0.6 mm$^3$. After the specimens were ground and electropolished in a solution of 40% $H_2SO_4$ and 60% $H_3PO_4$ at 32 °C, they were ultrasonically cleaned in acetone, methanol, and distilled water, progressively. Then, the specimens were loaded into the chamber of HCD ion-plating equipment for TiN deposition.

The specimens were first heated to the desired temperature. Then, they were ion bombarded by an argon glow discharge for ten minutes. The deposition was carried out at a partial pressure of 0.11 Pa for both argon and nitrogen. The titanium source material was evaporated by the HCD electron beam gun. The substrates of polished stainless steel with starting temperatures from 275 to 350 °C were at a bias voltage of –80 V. The HCD gun power was controlled by keeping a constant ion current at 200 A with varying voltage from 20 to 25 V. The final TiN film thickness is ~1 μm, which was measured using a scanning electron microscope (SEM).

Titanium nitride coated 304 SS specimens were prepared for transmission electron microscopy (TEM) study. After being ground to the thickness of ~80 to 90 μm, the specimens were punched into 3 mm diameter disks using a manual punch. The specimens were further dimpled down to ~5 to 10 μm thickness with a dimple grinder. Finally, thinning of the specimens was performed by a precision ion miller. Some TEM specimens were dimpled from both sides of the specimen. On the side of TiN film, the dimpling depth was controlled to be less than film thickness. Then the specimen was dimpled on the reverse (substrate) side. After dimpling, the specimens were further thinned by an ion miller to reveal the inside microstructure of TiN film.

The crystallographic preferred orientations of the TiN film were identified by x-ray diffraction (XRD) with copper-*K*α radiation. The hardness of the TiN film was measured by an ultramicrohardness tester. To facilitate the measurement of the indentation, a Knoop indentor was employed, and the testing load was 5 gf. Composition of the TiN coating layer was determined using x-ray photoelectron spectroscopy (XPS).

## 3. Results and Discussion

### *3.1 Microstructure of TiN*

Figure 1(a) shows the grain morphology in the surface layer of a TiN film. The grain size is ~80 to 100 nm and was measured

**C.T. Chen**, **Y.C. Song**, **G.-P. Yu**, and **J.-H. Huang,** Department of Engineering and System Science, National Tsing Hua University, Hsinchu, Taiwan 300, R.O.C.

from TEM micrographs using the linear intercept method. Figure 1(b) shows that the selection area diffraction exhibits a ring pattern. This indicates that the grains in the surface layer are polycrystalline with a random orientation. Figure 1(c) shows the inner microstructure of TiN film close to the 304 SS substrate. The grain size in Fig. 1(c) is <20 nm, which is apparently smaller than the grain size in the surface layer. Figure 1(d) is the selection area diffraction pattern of Fig. 1(c). Again, a ring pattern is observed, and the rings are more distinct than those in Fig. 1(b). This also indicates that the grain size in the inner layer is much smaller than the grain size in the surface layer. Figure 2 shows a high-resolution transmission electron microscopy (HRTEM) image of nanograins with an average diameter of ~10 nm for the same specimen in Fig. 1. In fact, the grain sizes of the TiN film in this study are generally in nanometer range.

The nanometer size grains may be due to the effect of ion bombardment, which affects the nucleation sites on the substrate (Ref 8-10). Because HCD ion plating has a high-ionization probability, a large number of fast ions bombard the substrate surface under bias voltage. Consequently, the substrate surface is disturbed, and many nucleation sites are created during the process. As titanium and nitrogen atoms condense and react on the substrate surface, TiN grains are easy to nucleate but difficult to grow because too many grains are nucleated simultaneously. These grains can impede each other to grow in their sites. As a result, nanometer grains are produced. This ion-bombardment enhanced nucleation mechanism

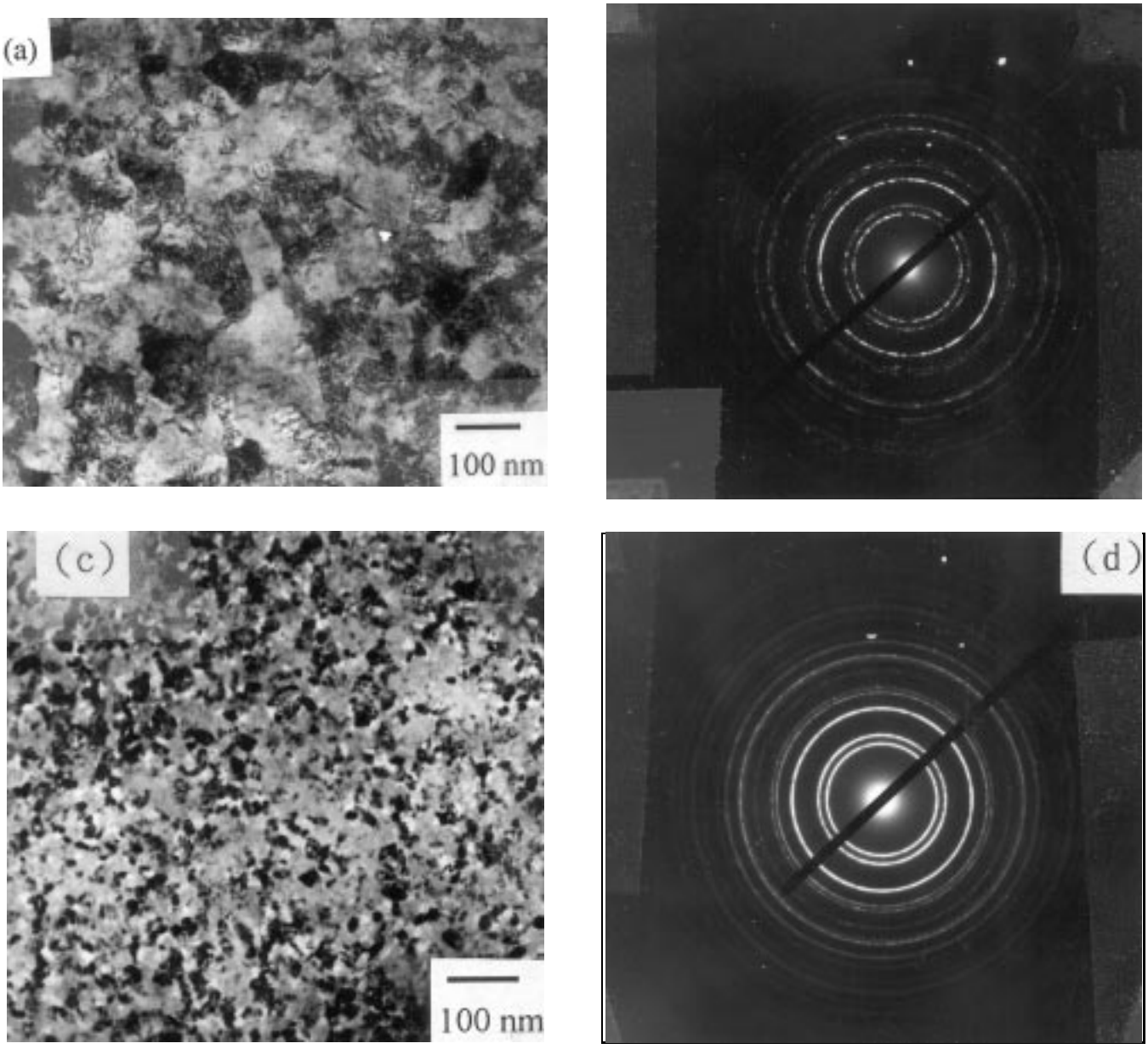


**Fig. 1** (a) Bright field image of the surface layer of a titanium nitride film. (b) Selection area diffraction pattern of the surface layer. (c) Bright field image of inner layer close to the substrate of a titanium nitride film. (d) Selection area diffraction pattern of the inner layer

is believed to occur throughout the plating process. The presence of nanometer-size grains in the surface layer of TiN film is evidence to support the previous argument.

Figure 1(a) and (c) also indicate that the TiN grains are enlarged during the deposition process. This observation is consistent with the revised structure zone model proposed by Messier et al. (Ref 11). In their model, the grain size in the film increases with increasing film thickness, which is attributed to the synergistic effect of thermal and bombardment induced mobility. The physical structure of a thin film is related to mobility of the adatoms at the growing film surface. During film deposition, the substrate and the deposited film continuously receive energy from the incoming ions. This input energy not only raises the temperature of the specimen, but also increases the mobility of the adatoms or molecular species. Therefore, grain growth is more significant as film thickness increases.

**Table 1 Summary of the experimental results of compositions, texture coefficient, and hardness of TiN coating specimens**

| Specimen No. | N/Ti ratio | Texture coefficient | Hardness, kgf/mm$^2$ |
|---|---|---|---|
| 1 | 1.245 | 39.46 | 1980 |
| 2 | 1.117 | 2.07 | 2022 |
| 3 | … | 11.14 | 1103 |
| 4 | 1.12 | 16.06 | 1716 |
| 5 | 1.332 | 0.69 | 416 |
| 6 | 1.298 | 172.65 | 2243 |
| 7 | 0.902 | 3.71 | 2144 |

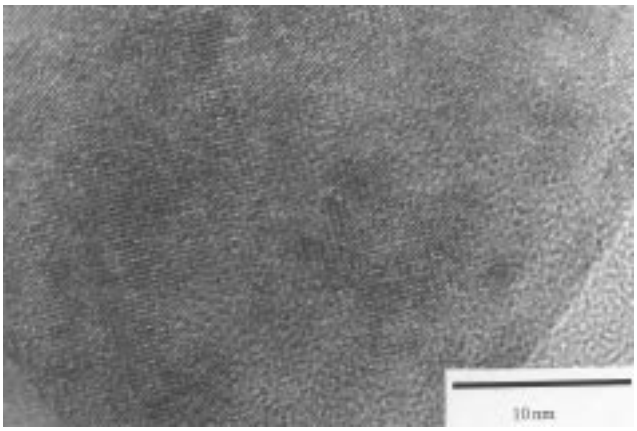


**Fig. 2** HRTEM image of titanium nitride nanograins

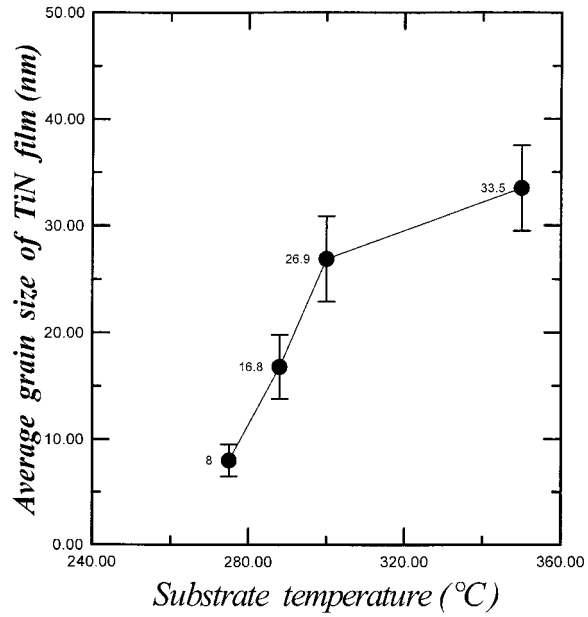


**Fig. 3** Average grain size vs. starting substrate temperature on the titanium nitride surface layer

The average grain size increases with increasing substrate temperature, $T_s$, from 8 nm at $T_s$ = 275 °C to 33.5 nm at $T_s$ = 350 °C, as shown in Fig. 3. At higher temperatures, because of the higher bulk and surface diffusion rate, adatoms and molecular species can migrate a larger distance, which leads to the formation of coarser grains.

Figure 4 shows the microstructure close to the 304 SS substrate. Slip steps can be observed in the grain of this region. The slip steps suggest that the formation of TiN film is accompanied with a very high compressive stress (Ref 12) and consequently results in plastic deformation in the metal substrate.

### *3.2 Preferred Orientation of TiN Film*

The preferred orientation of the TiN film was determined by XRD. Figure 5 shows a typical XRD pattern of 304 SS with TiN film. Two preferred orientations in TiN film, namely TiN(111) and TiN(200), are shown, which is consistent with previous observations (Ref 13-15). The major preferred orientation in the TiN film is TiN(111), which can be attributed to the fact that the (111) plane is the most close-packed surface with the lowest surface energy. The close-packed planes are also slow-growth planes, and such planes are known to survive at the expanse of fast-growth planes (Ref 16).To compare the relative strength of TiN(111), a texture coefficient is defined as:

$$\frac{\text{Peak intensity ratio TiN(111) / TiN(200) for specimen}}{\text{Peak intensity ratio TiN(111) / TiN(200) for powder specimen}}$$


**Fig. 4** Slip steps on 304 SS near titanium nitride film

The increase of texture coefficient that represents TiN(111) is more pronounced.

### *3.3 Hardness*

Table 1 summarizes the experimental results of composition, texture, coefficient, and hardness of TiN coating specimens. Figure 6 shows that the hardness of TiN film varies with the texture coefficient. The hardness of TiN film increases rapidly with texture coefficient between 0 and 40. Beyond a texture coefficient of 40, the hardness of TiN film levels off and reaches a value of ~2100 kgf/mm$^2$. This result clearly indicates that the hardness of TiN film is closely related to the texture of the film. However, the increase of the hardness can be from the variation of composition. For several deposition techniques, the maximum microhardness is reached for the composition $TiN_{x = 0.6}$ (Ref 1). From Fig. 7, the variation of N/Ti ratio from 0.902 to 1.332, the maximum hardness is at N/Ti = 1.298, and there is no relation between the N/Ti ratio and the (111) diffraction intensity. Figure 8 shows that the texture coefficient is not dependent on the N/Ti ratio.

If the effect of preferred orientation is considered, the specimen having a higher degree of TiN(111) texture will be harder than specimens having TiN(200) or other orientation. This can be explained from the relationship between preferred orientation and the resolved shear stress on the slip systems of TiN,

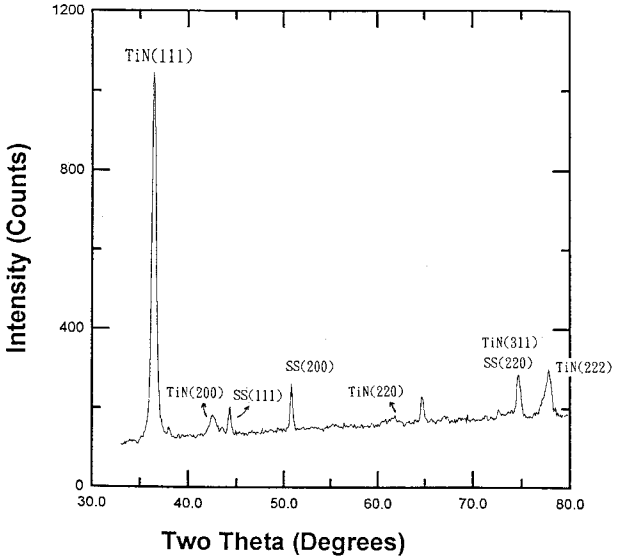


**Fig. 5** Typical x-ray diffraction pattern of 304 SS with titanium nitride film

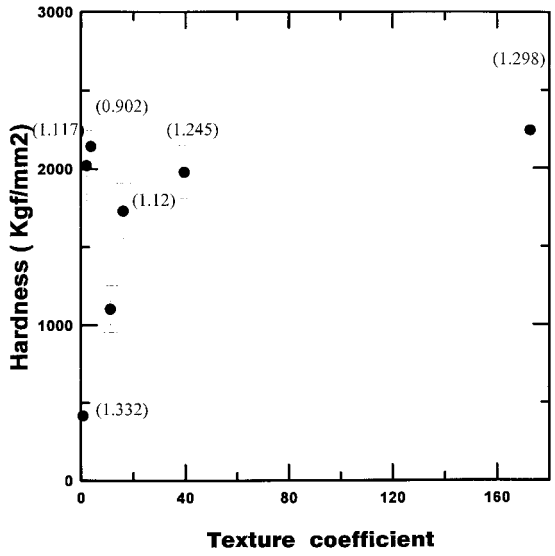


**Fig. 6** Texture coefficient of film vs. hardness of titanium nitride film

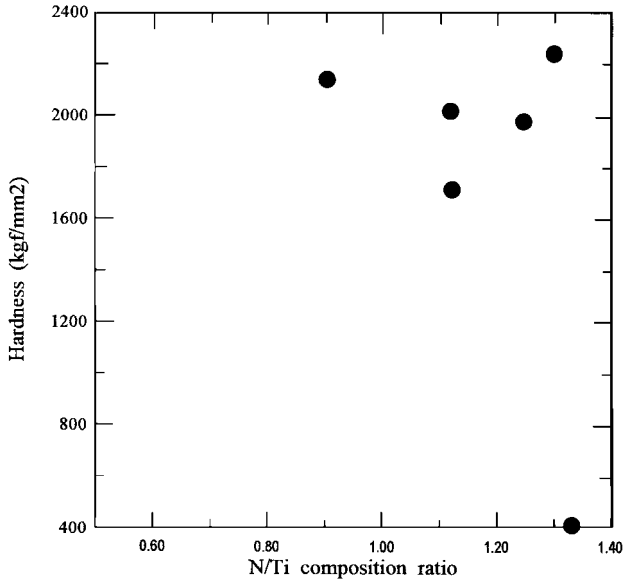


**Fig. 7** Hardness vs. composition of titanium nitride film

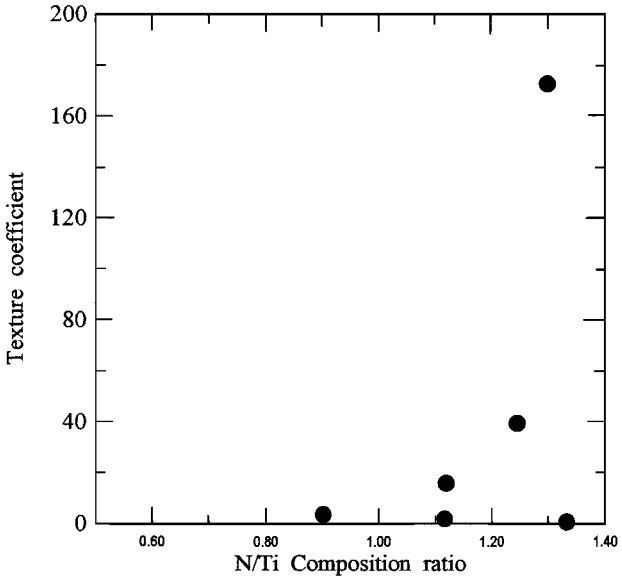


**Fig. 8** Texture coefficient vs. composition of titanium nitride film

**Table 2 Schmid factors of the slip systems in TiN as the external force in a direction of <111>**

| Cos φ | Cos θ | Schmid factor, Cos φ Cos Θ | Slip system of TiN |
|---|---|---|---|
| 0 | $2/\sqrt{6}$ | 0 | (110)[1$\bar{1}$0]<br>(110)[$\bar{1}$10]<br>(101)[10$\bar{1}$]<br>(101)[$\bar{1}$01]<br>(011)[01$\bar{1}$]<br>(011)[0$\bar{1}$1] |
| $2/\sqrt{6}$ | 0 | 0 | (1$\bar{1}$0)[110]<br>($\bar{1}$10)[110]<br>(10$\bar{1}$)[101]<br>($\bar{1}$01)[101]<br>(01$\bar{1}$)[011]<br>(0$\bar{1}$1)[011] |

<110> {110} (Ref 17). Table 2 lists all slip systems and Schmid factors for a TiN single crystal with an external force in a [111] direction. For the specimen having TiN(111) texture, the Schmid factor on all slip systems is zero when the external force is perpendicular to the (111) plane; that is, no resolved shear stress will be applied on slip systems. As a result, it is very difficult to induce plastic deformation, and thus higher hardness is measured. The results in Fig. 6 are consistent with the rationale. In the range of texture coefficient from 0 to 40, because the extent of TiN(111) preferred orientation increases, the hardness of the film increases. As the texture coefficient exceeds 40, the film hardness increases slightly and almost levels off. This implies that the grains in TiN film are uniformly oriented to [111] direction as the texture coefficient exceeds 40, such that the film hardness is close to the hardness of single crystal film in [111] direction, ~2300 kgf/mm$^2$ (Ref 18).

The hardness of TiN film can also be related to the intrinsic factors such as stoichiometry and defect concentration. For the film with large grain size and low dislocation density, the hardness of TiN is mainly determined by Pierls stress and, hence, the bond strength (Ref 1). The bond strength depends on parameters such as the stoichiometry and the vacancy concentration. In the present study, because the TiN film has nanometer grains, the contribution from Pierls stress can be reasonably neglected.

## 4. Conclusions

- Preferred orientations of the TiN film are TiN(111) and TiN(200). TiN(111) is the major preferred orientation.
- Hardness of the TiN film is contributed from TiN(111) texture. If the texture coefficient is <40, the film hardness increases with increasing texture coefficient; at >40, the TiN film hardness levels off and is closed to a value of the hardness of TiN single crystal film in [111] direction, 2300 kgf/mm$^2$.
- Grain size in TiN film is within nanometer range.


### Acknowledgments

The authors thank Professor F.S. Shieu for help with the TEM study. They also appreciate Dr. F.L. Chen for his help with HRTEM at the Materials Science Center of Tsing Hua University. This research was funded by the Atomic Energy Council of the Republic of China under contract AEC 842001NRD011 and the National Science Council of the Republic of China under contract NSC 85-2216-E-007-034.


### References


1. J.-E. Sundgren, *Thin Solid Films*, Vol 128, 1985, p 21
2. C. Quaeyhaegens, J. D'haen, L.M. Stals, M. Van Stappen, F. Bodart, and G. Terwagne, *Surf. Coat. Technol.*, Vol 61, 1993, p 227
3. K. Xu, J. Chen, R. Gao, and J. He, *Surf. Coat. Technol.*, Vol 58, 1993, p 37
4. M.G. Hocking, V. Vasantasree, and P.S. Sidky, *Metallic and Ceramic Coatings: Production, High Temperature Properties and Applications*, John Wiley & Sons, 1989
5. J.S. Colligon, H. Kheyrandish, L.N. Lesnevsky, A. Naumkin, A. Rogozin, I.J. Shkarban, L. Vasilyev, and V.E. Yurasova, *Surf. Coat. Technol.*, Vol 70, 1994, p 9
6. D.M. Mattox, *Deposition Technologies for Films and Coatings*, R.F. Bunshan, Ed., Noyes, New York, 1982
7. D.G. Teer, *Coatings for High Temperature Applications*, E. Lang, Ed., Applied Science, New York, 1983
8. M. Marinov, *Thin Solid Films*, Vol 46, 1977, p 267
9. V.O. Babaev, J.V. Bykov, and M.B. Guseva, *Thin Solid Films*, Vol 38, 1976, p 1
10. L. Pranevicius, *Thin Solid Films*, Vol 63, 1979, p 77
11. R. Messier, A.P. Giri, and R.A. Roy, *J. Vac. Sci. Technol. A*, Vol 2 (No. 2), 1984, p 500
12. C.A. Davis, *Thin Solid Films*, Vol 226, 1993, p 30
13. C.F. Ai, M.T. Chen, C.L. Moh, J.Y. Wu, and J.S. Su, *J. Vac. Soc. Roc.*, Vol 2 (No. 3), 1989, p 33
14. W. Posadowski, L. Krol-Stepniewska, and Z. Ziolowski, *Thin Solid Films*, Vol 62, 1979, p 347
15. A.K. Suri, R. Nimmagadda, and R.F. Bunshan, *Thin Solid Films*, Vol 72, 1980, p 529
16. J.A. Thornton, *Ann. Rev. Mater. Sci.*, Vol 7, 1977, p 239
17. Z. Wokulski, *Phys. Stat. Solidi (a)*, Vol 120, 1990, p 175
18. B.O. Johansson, J.-E. Sundgren, J.E. Greene, A. Rockett, and S.A. Barnett, *J. Vac. Sci. Technol. A*, Vol 3, (No. 2), 1985, p 303